

Kinetics of thermal degradation and thermo-oxidative degradation of conductive styrene-butadiene rubber-carbon black composites

G. T. Mohanraj · T. Vikram · A. M. Shanmugharaj ·
D. Khastgir · T. K. Chaki

Received: 25 November 2004 / Accepted: 28 September 2005 / Published online: 9 May 2006
© Springer Science+Business Media, LLC 2006

Abstract The kinetics of the thermal degradation and thermo-oxidative degradation of conductive styrene-butadiene rubber (SBR)-carbon black composites were investigated using thermogravimetric analysis both in nitrogen and oxygen atmospheres. Experiments were carried out at heating rates of 5, 10, 15 and 20 °C/min in both the atmospheres. Friedman method, Kissinger method, Flynn–Wall–Ozawa method and Coats–Redfern method have been used to determine the activation energies of degradation. The invariant kinetic parameters using the IKP method were also determined. The results showed that the thermal stability of the composites in pure nitrogen is higher than that in air atmosphere and the increase in filler loading was found to increase the thermal stability in nitrogen atmosphere. The probable degradation mechanisms of the polymer in both the atmospheres were evaluated based on Fourier Transform Infra Red Spectroscopy (FT-IR) studies.

Introduction

Conductive polymer composites have found use in numerous high technology applications in aerospace

industries, in modern electrical components and devices [1–5]. Thermal stability is one of the properties that can determine processing and application of materials. The practical use of polymeric materials requires knowledge of their thermal lifetime corresponding to a certain end-point criterion and the operating temperature.

Though, there are many works available on the kinetics of Styrene-butadiene rubber (SBR) [6–9], as far as the authors know, no investigation has been found in the literature on the kinetics of SBR filled with conductive carbon black (CCB), especially with the invariant kinetic parameter (IKP) method [10]. In general the thermal decomposition of polymers and filled polymers are studied in nitrogen atmosphere but the situation that a polymer is exposed to air is more common than in nitrogen during real processing and application. Several researchers have investigated the thermal degradation of polymers in both nitrogen and oxygen atmospheres [11–13]. In this paper the kinetics of degradation of SBR filled with CCB both in nitrogen and oxygen atmosphere are reported. The activation energies obtained from various isoconversional kinetic methods, the IKPs and the probable mechanisms that the degradation follows in nitrogen and air are presented in this paper.

Experimental

Materials

Styrene-butadiene rubber (SBR-1502, styrene content 23.5%, ML_{1+4} 100 °C, 51) procured from Synthetic and Chemicals Ltd., Barielley, India and CCB {Vulcan XC-72} procured from Cabot India Ltd were used for the preparation of the composites. The rubber, carbon black and the

G. T. Mohanraj · T. Vikram · D. Khastgir · T. K. Chaki (✉)
Rubber Technology Centre, Indian Institute of Technology,
Kharagpur 721302, India
e-mail: tapan@rtc.iitkgp.ernet.in

A. M. Shanmugharaj
Department of Chemical Engineering, College of Environment
and Applied Chemistry, Kyung Hee University, Yongin, South
Korea

various ingredients were mixed in a two roll mill. A standard formulation shown in Table 1 was used for mixing in which the filler loading was varied from 10 to 60 phr. The composites were cured at 150 °C in an electrically heated press to optimize the cure time as obtained from rheographs (Monsanto Rheometer R100).

Thermogravimetric measurement

Thermogravimetric measurements of the composites were conducted with a TA Q 50 thermogravimetric analyzer at heating rates of 5, 10, 15, 20, °C/min in a range of ambient temperature to 800 °C under a steady flow of nitrogen and oxygen.

Fourier transform infrared spectroscopy (FT-IR)

In order to have an idea of the process of degradation, samples containing very dilute solutions of pure SBR in Toluene were heated on KBr pellets in a furnace under the same conditions as in TGA and held at different temperatures 325, 350 and 400 °C isothermally for different times 2, 3 and 5 min. IR spectra of the degraded samples (on KBr-pellets) were obtained in a Perkin-Elmer (Model: Spectrum RX I) FT-IR spectrophotometer. All the results given in this paper are the averages of two measurements, with 32 scans for each measurement at a resolution of 4 cm⁻¹.

Kinetic methods

Friedman method

This is an isoconversional differential method based on the following equation [14]

$$\ln \beta d\alpha/dT = \ln A + \ln f(\alpha) - E/RT \quad (1)$$

where α = fraction of conversion, β = heating rate in °C, A = pre-exponential factor, T = temperature in °C,

Table 1 The formulation used for the preparation of the composites

Ingredients	Loading (phr)
SBR 1502	100.0
Zinc oxide	5.0
Stearic acid	1.5
Antioxidant TQ	1.0
Vulcan XC-72	10–60
Process oil	1–7
MBTS	1.0
TMT	0.2
Sulfur	2.0

E = activation energy in kJ/mol, R = universal gas constant, $f(\alpha)$ = algebraic expression for differential methods.

For α = constant, $\ln(\beta d\alpha/dT)$ vs. $1/T$, obtained from thermograms recorded at several heating rates yields a straight line whose slope allows evaluation of the activation energy.

Kissinger–Akahira–Sunose method (KAS method)

This is an isoconversional integral method based on the following equation [15]

$$\ln \beta/T^2 = \ln AR/Eg(\alpha) - E/RT \quad (2)$$

where $g(\alpha)$ = algebraic expression for integral methods.

For α = constant, $\ln(\beta/T^2)$ vs. $1/T$, obtained from thermograms recorded at several heating rates yields a straight line whose slope allows evaluation of the activation energy.

Flynn–Wall–Ozawa method (FWO method)

This is an isoconversional integral method based on the following equation [16–18]

$$\ln \beta = \ln AE/Rg(\alpha) - 5.331 - 1.052E/RT \quad (3)$$

For α = constant, $\ln \beta$ vs. $1/T$, obtained from thermograms recorded at several heating rates yields a straight line whose slope allows evaluation of the activation energy.

Coats–Redfern method (CR method)

This method uses a single heating rate and various conversion functions and gives idea about the degradation mechanism follows along with the activation energy (E) and the pre-exponential factor (A) values. Its based on the following equation [19],

$$\begin{aligned} \ln g(\alpha)/T^2 &= \ln [AR/\beta E(1 - 2RT/E)] - E/RT \\ &\simeq \ln AR/\beta E - E/RT \end{aligned} \quad (4)$$

The curve $\ln g(\alpha)/T^2$ vs. $1/T$, obtained from thermograms recorded at a single heating rate yields a straight line whose slope and intercept allows the evaluation of activation energy and pre-exponential factor respectively. Also the best fitting model of conversion function [$g(\alpha)$] gives the probable mechanism for by the degradation of the samples.

The IKP method

The IKP method is based on the observation that the same experimental curve $\alpha = \alpha(T)$ can be described relatively

correctly by several functions of conversion and, for a single TG curve, the values of the activation parameters, obtained for various analytical forms of $g(\alpha)$, can be correlated through the relation of the compensation effect, given by

$$\ln A_v = \alpha^* + \beta^* E_v \tag{5}$$

where A_v and E_v are obtained from the methods (here CR method) using single heating rate for various conversion functions and α^* and β^* are the compensation effect parameters. The straight lines $\ln A_v$ vs. E_v for several heating rates intersect in a point which corresponds to the true values of A and E and were called by Lesnikovich and Levchik [20] as invariant activation parameters (A_{inv} , E_{inv}) which are independent of conversion and specific to a particular system. Variations of the experimental conditions actually cause a region of intersection in the space (A , E). For this reason the evaluation of the invariant activation parameters can be performed using the relation [5],

$$\alpha^* = \ln A_{inv} - \beta^* E_{inv} \tag{6}$$

Thus, the plot α^* vs. β^* is actually a straight line whose parameters allow evaluating the invariant activation parameters.

Results and discussions

Thermal degradation (nitrogen atmosphere)

Analysis of thermograms

The composites of SBR with carbon black becomes semi-conductive only after the addition of 20 phr of carbon black and the percolation limit was found to be around 30 phr [21]. The kinetics of these conductive composites alone are investigated and reported. The TG and DTG curves corresponding to the thermal degradation of neat SBR and the composites of SBR containing 20, 30, 60 phr of carbon black in nitrogen atmosphere at the heating rate of 20 °C/min are shown in Figs. 1 and 2 respectively.

It can be observed that with increase in filler loading the amount of residue is increasing and it is because in nitrogen atmosphere only polymer and lower molecular weight ingredients like plasticizer, stearic acid undergoes the thermal degradation whereas carbon black remains unaffected. The same trend is found at all the heating rates. Due to this large amount of residue present in 60 phr composite the kinetics were studied only up to the conversion (α) of 0.5 for achieving a good comparison with other composites. Also it was observed that with increase in heating rate the

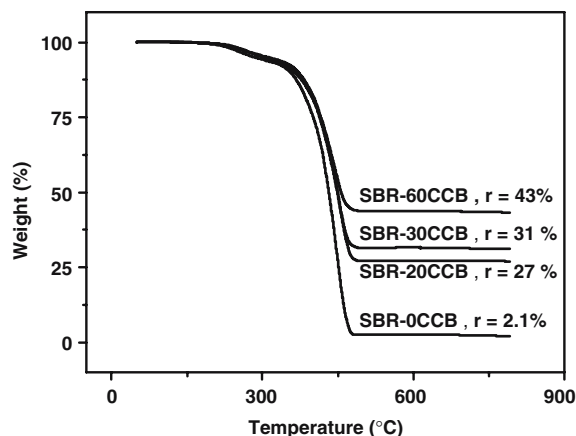


Fig. 1 Thermogravimetric curves (TG) of neat SBR and SBR composites filled with 20, 30, 60 phr of CCB in nitrogen atmosphere at 20 °C/min

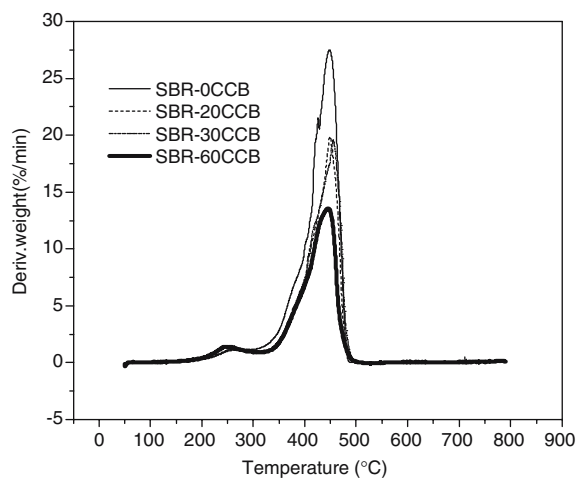


Fig. 2 Derivative Thermogravimetric curves (DTG) of neat SBR and SBR composites filled with 20, 30, 60 phr of CCB in nitrogen atmosphere at 20 °C/min

onset of degradation becomes slower, this is because the polymer gets exposed to heat more in slow heating rates than the higher ones. This is also reflected in the activation energy values obtained using CR method. From the DTG curves, it was found that all the composites exhibits two degradation steps. The degradation at low temp (around 260 °C temp.) corresponds to the volatilization of low molecular weight substances like plasticizers. The second step around 320 °C corresponds to the degradation of SBR, from the idea of already published data [6–9] and the kinetics of this polymer degradation step alone is evaluated.

Kinetics of thermal degradation

The expressions for the differential function $f(\alpha)$ and the integral function $g(\alpha)$ for some of the most common

mechanisms operating in solid state reactions are listed in Table 2.

The values of E , the activation energy and the corresponding correlation coefficients (r) for the polymer degradation in the composites obtained by Friedman, Flynn Wall Ozawa and Kissinger are included in Tables 3–5 respectively. From a careful observation of Table 3, it is clear that the values of E vary with conversion for all the composites considered. It can be seen that for the composites containing 20 and 30 phr of carbon black the value of E is almost constant or independent of conversion in the range of α from 0.2 to 0.5. In all the cases, activation energy increases with the increase in degree of conversion and it is almost constant at higher conversions for 20 and 30 phr loaded SBR vulcanizates. However, for 60 phr loading of CCB, the activation energy initially increases upto conversion of 0.2 and above which it decreases and then remains constant with further increase in alpha (0.3–0.5). Whenever filler is added into

a polymer, the interaction between polymer and filler may lead to many processes like bound rubber formation, rubber shell formation, occlusion and filler networking. Based on the nature of filler, polymer and also the amount of filler, one or many of the processes above can take place and have an effect on the degradation of the polymer [22–24]. In the case of low filler loading CCB forms a carbon black network which is responsible for the conduction of heat through this networks and thereby leads to degradation. However, at high filler loading (60 phr) along with the conductive networks, rubber forms a shell due to immobilized rubber layer around the filler aggregates that restricts the degradation initially and thereby improves the activation energy [22]. However, at higher conversion, the shell gets degrade that leads to the contact between the networks and thereby decreases the activation energy. For the composites containing 60 phr of black the activation energy seems to be varying much with the conversion.

Table 2 Expressions for $f(\alpha)$ and $g(\alpha)$ functions for some of the common mechanisms operating in the solid state reactions

Mechanism	Symbol	$f(\alpha)$	$g(\alpha)$
Reaction order model	Fn	$(1-\alpha)^n$	$-\ln(1-\alpha)$, for $n = 1$ $1-(1-\alpha)^{(-n+1)}/-n+1$, for $n \neq 1$
Random nucleation and growth of nuclei (Avrami–Erofeev equation)	An	$n(1-\alpha)[- \ln(1-\alpha)]^{(1-1/n)}$	$[- \ln(1-\alpha)]^{1/n}$
One-dimensional diffusion (parabolic law)	D1	$\frac{1}{2}\alpha$	α^2
Two-dimensional diffusion (bidimensional particle shape)	D2	$1/[- \ln(1-\alpha)]$	$(1-\alpha) \ln(1-\alpha)+\alpha$
Prout–Tompkins	B1	$\alpha(1-\alpha)$	$\ln(\alpha/1-\alpha)$
Power law	Pn	$n(\alpha)^{(n-1)/n}$	$\alpha^{1/n}$
Exponential law	E1	α	$\ln \alpha$

Table 3 Value of the activation energy obtained by means of Friedman method for SBR-CCB composites (N₂ atmosphere)

Conversion (%)	SBR-20CCB		SBR-30CCB		SBR-60CCB	
	E (kJ/mol)	$-r$	E (kJ/mol)	$-r$	E (kJ/mol)	$-r$
0.1	224.7	0.99	244.0	0.99	304.2	0.97
0.2	253.1	0.99	268.5	1.0	314.0	0.99
0.3	258.0	0.99	262.8	1.0	279.2	0.99
0.4	253.6	0.99	251.0	0.99	278.9	1.0
0.5	258.6	0.99	255.9	1.0	274.2	0.99

Table 4 Value of the activation energy obtained by means of FWO method for SBR-CCB composites (N₂ atmosphere)

Conversion (%)	SBR-20CCB		SBR-30CCB		SBR-60CCB	
	E (kJ/mol)	$-r$	E (kJ/mol)	$-r$	E (kJ/mol)	$-r$
0.1	218.5	0.99	212.9	0.99	267.3	0.91
0.2	218.5	0.99	218.5	0.99	362.8	0.93
0.3	277.9	0.99	268.5	0.99	277.9	0.99
0.4	271.3	0.91	277.9	0.99	277.9	1.0
0.5	277.9	1.0	277.9	0.99	268.5	0.99

Table 5 Value of the activation energy obtained by means of KAS method for SBR-CCB composites (N₂ atmosphere)

Conversion (%)	SBR-20CCB		SBR-30CCB		SBR-60CCB	
	<i>E</i> (kJ/mol)	<i>-r</i>	<i>E</i> (kJ/mol)	<i>-r</i>	<i>E</i> (kJ/mol)	<i>-r</i>
0.1	212.6	0.98	228.4	0.99	272.8	0.96
0.2	239.7	0.99	252.4	1.0	289.2	0.98
0.3	245.3	0.99	249.4	1.0	271.5	0.99
0.4	242.6	0.99	240.5	0.99	264.4	0.99
0.5	247.9	0.99	232.6	0.99	264.2	0.99

In order to apply the IKP method the conversion range in which the value of *E* is practically constant has to be determined and that has been done through all the above methods. So from the tables above it can be inferred that the conversion range where *E* is independent of α is 0.2 to 0.5 for SBR-20CCB and SBR-30CCB, while for SBR-60CCB it is 0.3–0.5.

For determining the compensation effect parameters (α^* , β^*) Coats–Redfern method has been applied in the range of conversion where *E* is independent of conversion. The kinetic models F1, F2, F5 and A0.5, A0.2 for which the straight lines plotted based on Eq. (4) which are characterized by *r* closer to 1, were considered. The values of activation parameters (*E*, ln *A*) obtained by means of CR method for SBR containing 20, 30 and 60 phr of carbon

black have been listed in Tables 6–8 respectively. It can be observed that the values of the activation parameters (*E*, ln *A*) depend on the kinetic model as well as on the heating rate. Some high differences among the values of the activation parameters corresponding to different kinetic models can be noted, although the correlation coefficients have appropriate values.

The values of *E* and ln *A* obtained by the use of CR method were used to determine the values of compensation parameters of α^* , β^* through the use of equation (5) and the values of IKPs *E*_{inv} and ln *A*_{inv} were evaluated by plotting α^* vs. β^* based on Eq. (6). The results are tabulated in the Table 9.

It can be very clearly seen that the values of *E*_{inv} increases with increase in the amount of filler loading as it

Table 6 Kinetic parameters evaluated from TG curves for thermal degradation of SBR-20CCB composites using Coats–Redfern method (N₂ atmosphere)

Model	$\beta = 5 \text{ }^\circ\text{C/min}$			$\beta = 10 \text{ }^\circ\text{C/min}$		
	<i>E</i> (kJ/mol)	ln <i>A</i> A (s ⁻¹)	<i>-r</i>	<i>E</i> (kJ/mol)	ln <i>A</i> A (s ⁻¹)	<i>-r</i>
F1	114.7	17.3	0.99	116.1	17.8	0.99
F2	142.4	22.6	0.99	144.1	23.1	0.99
F5	246.7	43.6	0.98	249.7	43.9	0.98
A0.5	240.8	39.2	0.99	243.7	39.6	0.99
	$\beta = 15 \text{ }^\circ\text{C/min}$			$\beta = 20 \text{ }^\circ\text{C min}$		
	<i>E</i> (kJ/mol)	ln <i>A</i> A (s ⁻¹)	<i>-r</i>	<i>E</i> (kJ/mol)	ln <i>A</i> A (s ⁻¹)	<i>-r</i>
F1	114.8	17.9	0.99	117.2	18.4	0.99
F2	143.6	23.1	0.99	145.5	23.7	0.99
F5	247.3	43.7	0.98	252.2	44.5	0.98
A0.5	241.3	39.3	0.99	246.2	40.2	0.99

Table 7 Kinetic parameters evaluated from TG curves for thermal degradation of SBR-30CCB composites using Coats–Redfern method (N₂ atmosphere)

Model	$\beta = 5 \text{ }^\circ\text{C/min}$			$\beta = 10 \text{ }^\circ\text{C/min}$		
	<i>E</i> (kJ/mol)	ln <i>A</i> A (s ⁻¹)	<i>-r</i>	<i>E</i> (kJ/mol)	ln <i>A</i> A (s ⁻¹)	<i>-r</i>
F1	121.3	18.5	1.0	118.8	18.3	0.99
F2	150.4	24.0	0.99	147.5	23.7	0.99
F5	253.9	41.6	0.98	255.7	45.2	0.99
A0.5	260.3	46.0	1.0	249.1	40.7	0.99
	$\beta = 15 \text{ }^\circ\text{C/min}$			$\beta = 20 \text{ }^\circ\text{C/min}$		
	<i>E</i> (kJ/mol)	ln <i>A</i> A (s ⁻¹)	<i>-r</i>	<i>E</i> (kJ/mol)	ln <i>A</i> A (s ⁻¹)	<i>-r</i>
F1	118.0	18.4	0.99	114.0	17.8	0.99
F2	146.6	23.8	0.99	141.8	23.0	0.99
F5	254.2	44.9	0.99	246.3	43.5	0.99
A0.5	247.7	40.5	0.99	239.9	39.1	0.99

Table 8 Kinetic parameters evaluated from TG curves for thermal degradation of SBR-60CCB composites using Coats–Redfern method (N₂ atmosphere)

Model	$\beta = 5 \text{ }^\circ\text{C/min}$			$\beta = 10 \text{ }^\circ\text{C/min}$		
	E (kJ/mol)	$\ln A A$ (s ⁻¹)	$-r$	E (kJ/mol)	$\ln A A$ (s ⁻¹)	$-r$
F1	111.1	16.4	0.99	110.8	16.7	0.99
F2	133.5	20.7	0.99	133.3	20.9	0.99
F5	215.6	37.6	0.99	215.3	37.6	0.99
A0.5	233.6	37.5	0.99	233.5	37.5	0.99
A0.2	283.6	37.5	0.99	283.5	37.5	0.99
Model	$\beta = 15 \text{ }^\circ\text{C/min}$			$\beta = 20 \text{ }^\circ\text{C/min}$		
	E (kJ/mol)	$\ln A A$ (s ⁻¹)	$-r$	E (kJ/mol)	$\ln A A$ (s ⁻¹)	$-r$
F1	104.8	15.9	0.99	105.4	16.2	0.99
F2	125.9	19.9	1.0	126.6	20.2	1.0
F5	202.9	35.6	0.99	204.0	35.9	0.99
A0.5	220.0	35.4	0.99	221.2	35.6	0.99
A0.2	280.0	35.4	0.99	281.2	35.6	0.99

Table 9 Values of compensation effect parameters and IKPs for the SBR-CCB composites (N₂ atmosphere)

β (K/min)	$-\alpha^*(A, \text{s}^{-1})$	β^* (mol/kJ)	$-r$	E_{inv} (kJ/mol)	$\ln A_{\text{inv}}$ (A _{inv} , s ⁻¹)
<i>SBR-20CCB</i>					
5	4.1896	0.1872	0.98	238.9	40.5
10	3.5233	0.1839	0.98		
15	3.1353	0.1829	0.98		
20	2.8406	0.1815	0.98		
<i>SBR-30CCB</i>					
5	4.1465	0.1868	0.99	266.2	45.6
10	3.4986	0.1843	0.98		
15	3.12	0.183	0.98		
20	2.8785	0.182	0.98		
<i>SBR-60CCB</i>					
5	3.6725	0.1831	0.98	300.5	51.3
10	2.9948	0.1802	0.98		
15	2.6177	0.1798	0.98		
20	2.318	0.1786	0.98		

was in the case of all isoconversional methods. The specialty of IKP method and the IKPs is that their values do not depend on conversion, the kinetic model, heating rate etc., and thus can be considered as a characteristic property of the particular system. The increase in E_{inv} with increase in filler loading represents the increase in thermal stability of the composites with increase in filler loading. From a careful observation of all the tables above it can be concluded that the composites of SBR containing 20 and 30 phr of carbon black exhibit a reaction order of 0.5. The composite containing 60 phr of carbon black has a lesser reaction order of 0.2 or it can be corroborated to zero order kinetics approximately. Eventhough in all the cases, the propagation of the nucleation leading to the degradation of the polymer chains depends on the availability of the active sites that are prone to degradation. With increase in filler loading, the active sites available for propagation of the degradation decrease due to the adsorption of the polymer molecules on the surface of filler particles, which increase with increase in filler loading. This is further confirmed

from the decrease in the reaction order from 0.5 (20& 30 phr loaded SBR) to 0.2 (60 phr loaded rubber) calculated based on Coats Redfern method.

Thermo-oxidative degradation (oxygen atmosphere)

Analysis of thermograms:

The TG and DTG curves corresponding to the thermal degradation of neat SBR and the composites of SBR containing 20, 30, 60 phr of carbon black in oxygen atmosphere at the heating rate of 20 °C/min are shown in Figs. 3 and 4 respectively.

It can be seen that in oxidative degradation there is no significant difference in the amount of residue obtained for all the composites as against the case of degradation in nitrogen. This is due to the oxidation of carbon black present in the composites forming carbon-di-oxide which escapes during the process of degradation and thus reducing the residue which constitutes the unaffected carbon

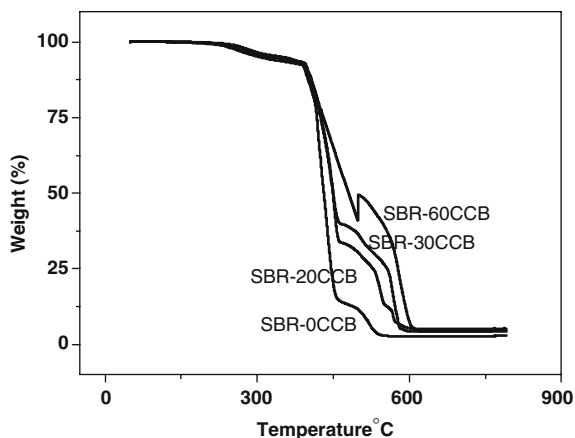


Fig. 3 Thermogravimetric curves (TG) of neat SBR and SBR composites filled with 20, 30, 60 phr of CCB in oxygen atmosphere at 20 °C/min

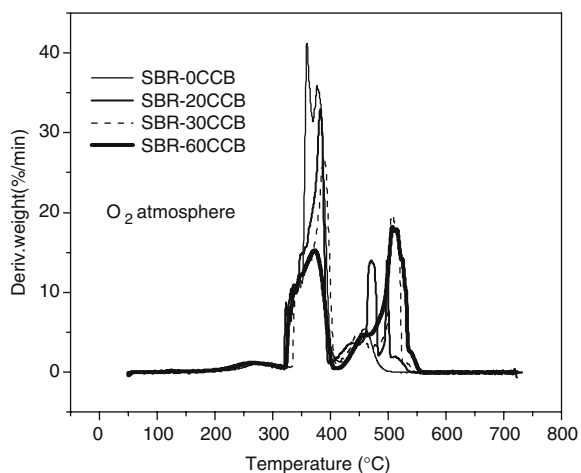


Fig. 4 Derivative Thermogravimetric curve (DTG) of neat SBR and SBR-CCB composites in oxygen atmosphere at 20 °C/min

black in the case of nitrogen. From Fig. 4 it can be seen that three degradation steps are present in the oxidative degradation of the composites. As before, the second step occurring around 320 °C corresponds to the polymer degradation whereas the third degradation step occurring around 500 °C corresponds to the oxidation of carbon

black into CO₂ and its evaporation from the composite system. The same case is observed in all the composites.

Kinetics of thermo-oxidative degradation

The values of *E*, the activation energy and the corresponding correlation coefficients (*r*) for the polymer degradation in the composites obtained by Friedman, Flynn Wall Ozawa and Kissinger are given in Tables 10–12. In order to apply the IKP method the conversion range in which the value of *E* is practically constant has to be determined and that has been done through all the above methods. So from the Tables 10–12, it can be inferred that the conversion range where *E* is almost constant in the range of α , 0.2–0.5 for all the composites.

For determining the compensation effect parameters (α^* , β^*) Coats–Redfern method has been applied in the range of conversion where *E* is independent of conversion. The kinetic models F1, F2, F5 and A0.5 for which the straight lines plotted based on Eq. (4) which are characterized by *r* closer to 1, were considered. The values of activation parameters (*E*, ln *A*) obtained by means of CR method of the composites containing 20, 30 and 60 phr of carbon black have been listed in Tables 13–15. The values of *E* and ln *A* obtained by the use of CR method were used to determine the values of compensation parameters of α^* , β^* through the use of Eq. (5) and the values of IKPs E_{inv} and ln A_{inv} were evaluated by plotting α^* vs. β^* based on Eq. (6). The results are tabulated in the Table 16.

By comparing the *E* values in Tables 10–12, which are obtained by isoconversional methods like FWO method, with that of the *E* values in Tables 13–15, obtained through it is instead of its values to that of other isoconversional methods. Thus, it can be said that the oxidative thermal degradation of all the composites follows first-order kinetics Also it can be observed from Table 16 that the activation energy values obtained in oxygen atmosphere are almost half of the activation energy values obtained in nitrogen atmosphere. This represents that the energy required to degrade the polymer in oxygen atmosphere is much lesser than in nitrogen and thus proves that the thermal stability of the composites is lesser in oxygen than nitrogen atmosphere. The reason behind this is that in the case of nitrogen

Table 10 Value of the activation energy obtained by means of Friedman method for SBR-CCB composites (O₂ atmosphere)

Conversion (%)	SBR-20CCB		SBR-30CCB		SBR-60CCB	
	<i>E</i> (kJ/mol)	– <i>r</i>	<i>E</i> (kJ/mol)	– <i>r</i>	<i>E</i> (kJ/mol)	– <i>r</i>
0.1	187.6	0.99	177.0	0.99	114.2	0.97
0.2	183.1	0.98	172.4	0.99	104.0	0.99
0.3	184.0	0.98	172.7	0.99	105.1	0.99
0.4	183.5	0.99	171.0	0.99	103.8	0.99
0.5	184.6	0.98	171.9	0.99	104.1	0.99

Table 11 Value of the activation energy obtained by means of Flynn–Wall–Ozawa method for SBR-CCB composites (O₂ atmosphere)

Conversion (%)	SBR-20CCB		SBR-30CCB		SBR-60CCB	
	<i>E</i> (kJ/mol)	<i>-r</i>	<i>E</i> (kJ/mol)	<i>-r</i>	<i>E</i> (kJ/mol)	<i>-r</i>
0.1	188.5	0.98	172.8	0.98	117.2	0.90
0.2	178.5	0.98	168.5	0.98	106.8	0.92
0.3	177.8	0.99	168.5	0.98	107.8	0.99
0.4	177.2	0.98	167.8	0.99	107.8	0.99
0.5	177.8	0.99	167.8	0.99	108.5	0.98

Table 12 Value of the activation energy obtained by means of KAS method for SBR-CCB composites (O₂ atmosphere)

Conversion (%)	SBR-20CCB		SBR-30CCB		SBR-60CCB	
	<i>E</i> (kJ/mol)	<i>-r</i>	<i>E</i> (kJ/mol)	<i>-r</i>	<i>E</i> (kJ/mol)	<i>-r</i>
0.1	182.6	0.98	188.3	0.99	112.5	0.96
0.2	179.1	0.98	172.1	0.99	108.2	0.99
0.3	177.0	0.99	173.3	0.99	107.0	0.99
0.4	177.1	0.99	171.5	0.99	106.9	0.99
0.5	177.2	0.99	170.9	0.99	106.4	0.99

Table 13 Kinetic parameters evaluated from TG curves for thermal degradation of SBR-20CCB composites using Coats–Redfern method (O₂ atmosphere)

Model	$\beta = 5 \text{ }^\circ\text{C/min}$			$\beta = 10 \text{ }^\circ\text{C/min}$		
	<i>E</i> (kJ/mol)	$\ln A A (\text{s}^{-1})$	<i>-r</i>	<i>E</i> (kJ/mol)	$\ln A A (\text{s}^{-1})$	<i>-r</i>
F1	181.9	15.1	0.99	180.1	15.8	0.99
F2	191.1	16.8	0.99	189.4	17.0	0.99
F5	205.3	23.1	0.98	203.7	22.9	0.98
A0.5	200.8	22.2	0.99	203.7	21.7	0.99
Model	$\beta = 15 \text{ }^\circ\text{C/min}$			$\beta = 20 \text{ }^\circ\text{C/min}$		
	<i>E</i> (kJ/mol)	$\ln A A (\text{s}^{-1})$	<i>-r</i>	<i>E</i> (kJ/mol)	$\ln A A (\text{s}^{-1})$	<i>-r</i>
F1	179.7	15.8	0.99	177.0	16.1	0.99
F2	188.6	17.0	0.99	185.5	17.6	0.99
F5	201.3	23.6	0.98	202.2	21.5	0.98
A0.5	201.3	22.3	0.99	206.2	21.1	0.99

Table 14 Kinetic parameters evaluated from TG curves for thermal degradation of SBR-30CCB composites using Coats–Redfern method (O₂ atmosphere)

Model	$\beta = 5 \text{ }^\circ\text{C/min}$			$\beta = 10 \text{ }^\circ\text{C/min}$		
	<i>E</i> (kJ/mol)	$\ln A A (\text{s}^{-1})$	<i>-r</i>	<i>E</i> (kJ/mol)	$\ln A A (\text{s}^{-1})$	<i>-r</i>
F1	177.1	14.5	1.0	176.2	14.4	0.99
F2	180.2	15.6	0.99	177.5	14.7	0.99
F5	200.1	21.1	0.99	199.0	21.2	0.99
A0.5	202.3	22.0	1.0	201.7	22.0	0.99
Model	$\beta = 15 \text{ }^\circ\text{C/min}$			$\beta = 20 \text{ }^\circ\text{C/min}$		
	<i>E</i> (kJ/mol)	$\ln A A (\text{s}^{-1})$	<i>-r</i>	<i>E</i> (kJ/mol)	$\ln A A (\text{s}^{-1})$	<i>-r</i>
F1	176.0	14.4	0.99	174.0	13.8	0.99
F2	176.6	14.8	0.99	171.8	14.1	0.99
F5	201.1	20.9	0.99	201.3	20.4	0.99
A0.5	201.7	23.5	0.99	202.1	24.1	0.99

atmosphere only thermal degradation takes place whereas in oxygen apart from thermal degradation oxidation of the polymer chains takes place decreasing its stability heavily. It is also found that with increase in filler loading the *E*

values decreases in oxygen as against an increase in the case of nitrogen atmosphere. This can be attributed to the entrapment of polymer chains by the filler aggregates making them smaller chains, which is also an outcome of

Table 15 Kinetic parameters evaluated from TG curves for thermal degradation of SBR-60CCB composites using Coats–Redfern method (O₂ atmosphere)

Model	$\beta = 5 \text{ }^\circ\text{C/min}$			$\beta = 10 \text{ }^\circ\text{C/min}$		
	$E \text{ (kJ/mol)}$	$\ln A A \text{ (s}^{-1}\text{)}$	$-r$	$E \text{ (kJ/mol)}$	$\ln A A \text{ (s}^{-1}\text{)}$	$-r$
F1	106.1	13.2	0.99	105.8	13.7	0.99
F2	123.2	14.7	0.99	123.3	14.9	0.99
F5	155.5	17.6	0.99	155.3	17.6	0.99
A0.5	163.3	17.7	0.99	164.1	16.0	0.99
Model	$\beta = 15 \text{ }^\circ\text{C/min}$			$\beta = 20 \text{ }^\circ\text{C/min}$		
	$E \text{ (kJ/mol)}$	$\ln A A \text{ (s}^{-1}\text{)}$	$-r$	$E \text{ (kJ/mol)}$	$\ln A A \text{ (s}^{-1}\text{)}$	$-r$
F1	104.8	15.9	0.99	105.4	16.2	0.99
F2	125.9	19.9	1.0	126.6	20.2	1.0
F5	152.9	17.0	0.99	154.0	16.8	0.99
A0.5	162.4	16.2	0.99	161.9	16.1	0.99

Table 16 Values of compensation effect parameters and IKPs for the SBR-CCB composites (O₂ atmosphere)

$\beta \text{ (K/min)}$	$-\alpha^* \text{ (A, s}^{-1}\text{)}$	$\beta^* \text{ (mol/kJ)}$	$-r$	$E_{inv} \text{ (kJ/mol)}$	$\ln A_{inv} \text{ (A}_{inv}\text{, s}^{-1}\text{)}$
<i>SBR-20CCB</i>					
5	2.86	0.148	0.99	184.5	38.2
10	2.51	0.142	0.99		
15	2.14	0.133	0.99		
20	2.06	0.132	0.99		
<i>SBR-30CCB</i>					
5	4.1465	0.146	0.99	176.0	34.5
10	3.4986	0.145	0.99		
15	3.12	0.143	0.99		
20	2.8785	0.142	0.99		
<i>SBR-60CCB</i>					
5	3.6725	0.139	0.98	107.3	29.7
10	2.9948	0.138	0.98		
15	2.6177	0.1375	0.98		
20	2.318	0.133	0.98		

polymer–filler interaction [22–24] which are easily degradable than the longer polymer chains through surface oxidation.

Mechanisms of degradation

In order to get an idea and also to verify the degradation of the styrene butadiene rubber, FTIR spectroscopy of the pure styrene butadiene elastomer is followed. Figure 5a shows the FTIR spectra of pure styrene butadiene rubber in the region 4000–450 cm⁻¹ taken at room temperature. The various peak positions and their assignments are summarized in Table 17. Figure 5b shows the FTIR spectra of pure styrene butadiene rubber in the region 2000–600 cm⁻¹ taken at four different temperatures of 28 °C, 325 °C, 350 °C and 400 °C, for 2 min under O₂ atmosphere using the same conditions as in TGA. The various peak positions and their assignments are summarized in Table 17.

During exposure of styrene butadiene rubber to heat at different temperatures in oxygen, changes are observed in the absorbances in the region of 1705 cm⁻¹ and 1604 cm⁻¹ indicating aerial oxidation and chain scission reactions.

Table 17 Peak position and assignment of peaks in the IR spectra of SBR rubber

Wave number (cm ⁻¹)	Functional group
3030	–CH stretching vibration of –CH groups
3068	–CH stretching vibration of olefinic group
2925, 2855	–CH stretching vibration of methylene groups
1490	>C=C< stretching of aromatic ring (styrene)
1604, 1599	>C=C< stretching for aliphatic olefinic group
1375	H–C–H bending vibration of methylene group
965	–C=C–H deformation for aliphatic unsaturation

The bond energy of labile hydrogens in the methylene linkage is about 377 kJ mol⁻¹. On thermal treatment, these hydrogens are split off, generating macro radicals on the carbon atoms of diene unit. On the other hand, these macro radicals either react with oxygen in air, resulting in formation of carbonyl groups or result in formation of double bonds. Various reactions showing the carbonyl group formation involving both styrene and butadiene units are mentioned in Schemes 1a and 1b. The occurrence of aerial

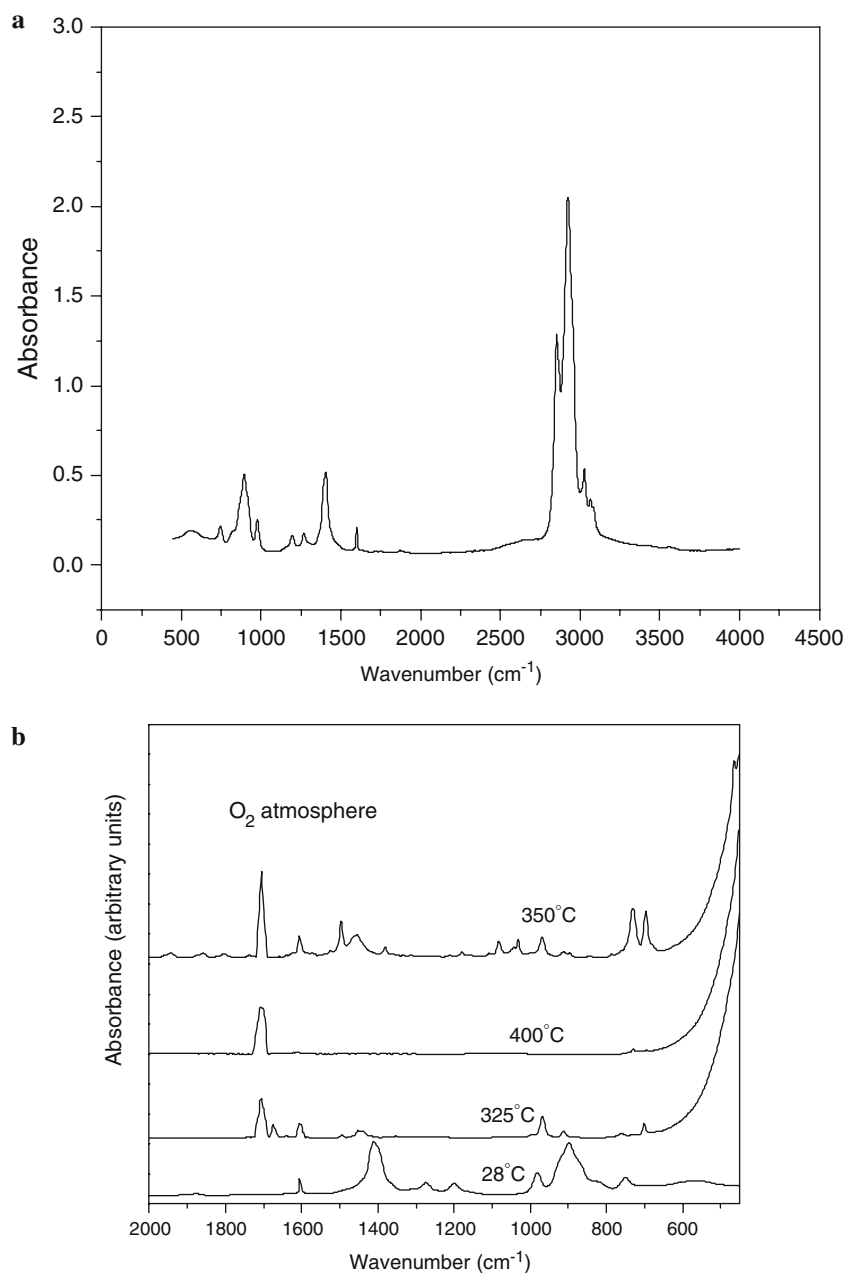
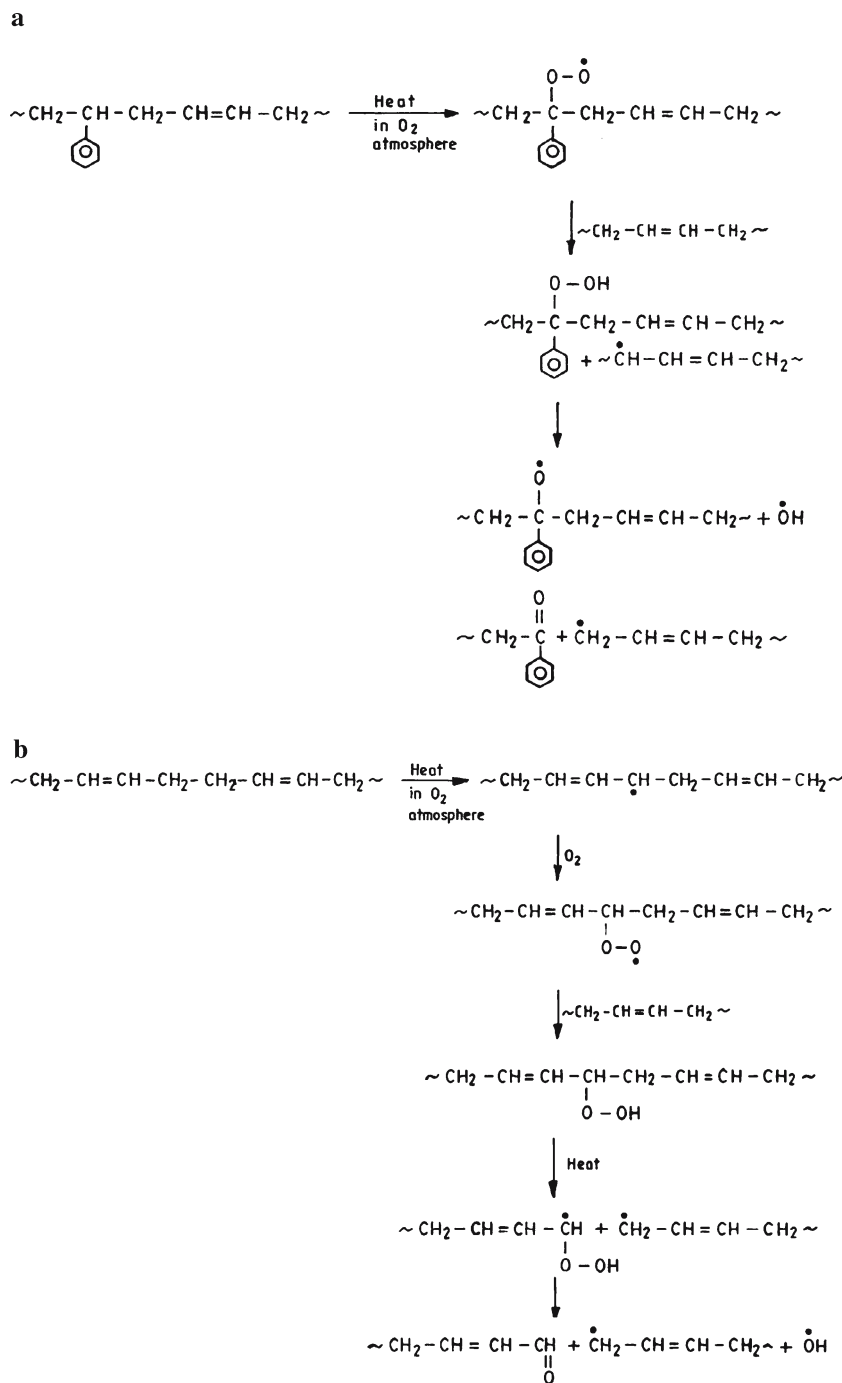


Fig. 5 (a) IR spectra of pure SBR in the region 4000–450 cm^{-1} taken at room temperature. (b) IR spectra of pure SBR in the region 2000–450 cm^{-1} heated at different temperatures (28–400 $^{\circ}\text{C}$) for a particular time of heating (2 min) in oxygen atmosphere

oxidation is also affirmed from the increase in peak heights at 1705 cm^{-1} at different temperatures (Fig. 6). The decrease in peak height in the case of 400 $^{\circ}\text{C}$ can be attributed to the dominance of competing reactions of chain scission compared to carbonyl group formation at that high temperature. It is fairly well known that polybutadiene is susceptible to O_2 attack even at room temperature. This reaction is accelerated by heat. Furthermore, from literature [25] it was found that two intensive absorption bands at 240 and 280 nm by UV spectroscopy were seen for SBR

during degradation, which is attributed to the formation of conjugated carbonyl groups. The chain scission resulting in unsaturation is also affirmed from the occurrence of peak at 1604 cm^{-1} which are due to the asymmetric stretching vibrations of the $\text{C}=\text{C}=\text{C}$ groups and vinyl groups respectively. This is due to the disproportionation reaction occurring in the unsaturation units in the elastomer (Scheme 2). Another work by Abu-Zeid and Youssef [26] on this system also suggests the formation of unsaturation on thermal treatment. A same behaviour is observed at different

Scheme 1 (a) Formation of carbonyl groups (oxidation) involving styrene units. (b) Formation of carbonyl groups (oxidation) involving butadiene units



temperature in nitrogen atmosphere. The formation of carbonyl groups due to aerial oxidation is avoided in nitrogen atmosphere. This is indicated by the absence of these peaks in this atmosphere (Fig. 7).

Scheme 2 shows a common mechanism of degradation only under heat which can take place in any atmosphere Scheme 1a and b shows the possible mechanism of degradation in oxygen atmosphere under heat. Thus, Scheme 2 represents the degradation mechanism in nitrogen atmo-

sphere whereas all the Schemes 1a, 1b, 2 together represent the degradation mechanism in oxygen atmosphere.

Conclusions

The increase in filler loading increased the activation energy of degradation in nitrogen atmosphere whereas decreased the activation energy in oxygen atmosphere. The

Scheme 2 Thermal degradation mechanism of SBR under oxygen/nitrogen atmospheres—Formation of unsaturations

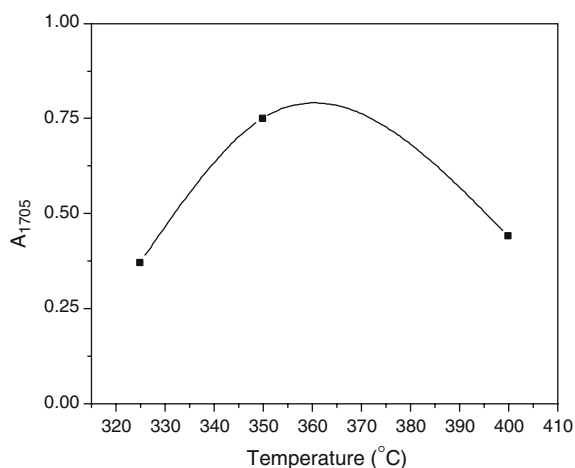
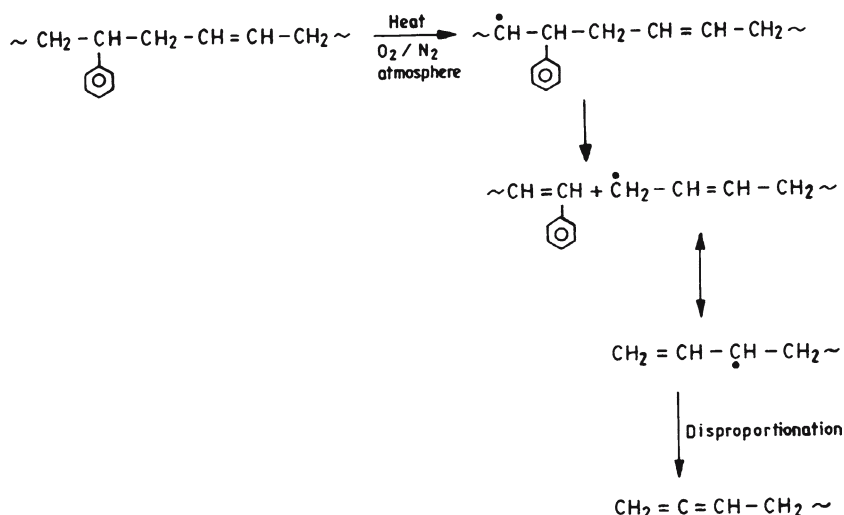


Fig. 6 Plot depicting the variation of the ratio of Peak Height due to C=O groups (1705 cm⁻¹) of SBR during degradation in oxygen atmosphere

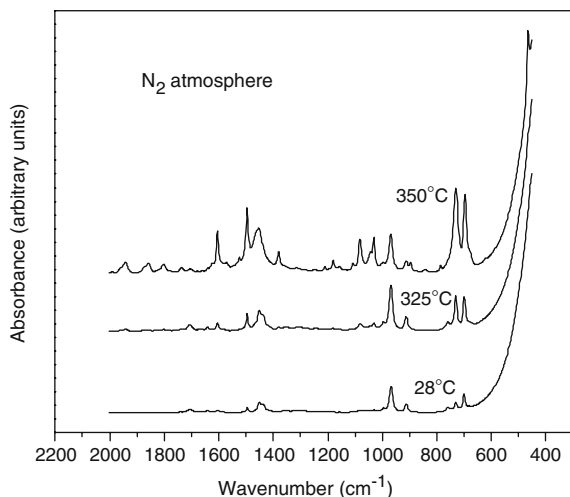


Fig. 7 IR spectra of pure SBR in the region 2000–450 cm⁻¹ heated at different temperatures (28–400 °C) for a particular time of heating (2 min) in nitrogen atmosphere

thermal stability of the composites is higher in nitrogen than in oxygen atmosphere. The composites were found to follow first-order kinetics in oxygen and in nitrogen showed fractional orders. The mechanisms of degradation of the polymer was established by FT-IR and were found to be characterized by carbonyl group formation along with increase in unsaturation during degradation in oxygen atmosphere against only the increase in unsaturation in nitrogen atmosphere.

Acknowledgements The authors thank the Indian Space Research Organization (ISRO), Bangalore for financial support of this work.

References

- Gupta RK (1988) Fibre reinforcements for composites materials. Elsevier, Amsterdam chap. 2
- Meyers MA (1985) Frontiers in materials technologies. Elsevier, Amsterdam, chap. 1
- Narkis M, Vaxman A (1984) J Appl Polym Sci 29:1639
- Kakizawa K (1986) Int Polym Sci Technol 13(2):40
- Chung DDL (2001) Carbon 39(2):279
- Cheon OS, Pyeong LH, Sung-Chul Yi, Ok YK (1999) J Fire Sci 17(5):362
- Cheon OS, Pyeong LH, Taik KH, Ok YK (1999) J Chem Eng 16(4):543
- Li KW, Deuk KS, Bum LS, Kwon HI (2000) J Ind Eng Chem (Seoul) 6(5):348
- Cheon OS, Chul JH, Taik KH (2003) J Chem Eng Jpn 36(8):1016
- Budrugaec P (2001) Polym degrad stab 74:125
- Wen-Yen C, Fa-Tai W, Leo-Wang C, Trong-Ming D, Ching-Yuan L (2000) Polym degrad Stab 67:223
- Katsikas L, Boskovic G, Velickovic SJ, Velickovic JS, Popovic IG (2000) Eur Polym J 36:1619
- Santhana Gopala Krishnan P, Vora RH, Veeramani S, Hong GS, Tai-Shung C (2002) Polym Degrad Stab 75:273
- Friedman HJ (1964) Polym Sci Part C 6:183
- Kissinger H (1957) Anal Chem 29:1702
- Flynn J, Wall L (1966) J Polym Sci B 4:323

17. Ozawa T (1965) Bull Chem Soc Jpn 38:1881
18. Flynn H, Wall LA (1967) Polym Lett 5:191
19. Coats A, Redfern J (1964) Nature 201:68
20. Lesnikovich AI, Levchik SV (1985) J Thermal Analysis 30:667
21. Mohanraj GT, Chaki TK, Chakraborty A, Khastgir D (2004) J Appl Polym Sci 92:2179
22. Donnet JB, Wong MJ (eds) (1993) Carbon black science & technology, 2nd edn. Marcel Dekker Inc., NY, Chap 9, p 295
23. Gonzalez AV, Veleza L (2004) Polym Degrad Stab 83:139
24. Ronaldo AC, Regina CRN, Vera LL (1996) Polym Degrad Stab 52:245
25. CR Acad Sco, Ser C 266:678 (1968)
26. Abu-Zeid ME, Youssef YA (1986) J Appl Polym Sci 31:1575